

# Tailoring Electromechanical Properties of Natural Rubber Vitrimers by Cross-Linkers

Khoa Bui, Alan M. Wemyss, Runan Zhang, Giao T. M. Nguyen, Cedric Vancaeyzeele, Frederic Vidal, Cedric Plesse, and Chaoying Wan\*



Cite This: <https://doi.org/10.1021/acs.iecr.2c01229>



Read Online

ACCESS |



Metrics & More

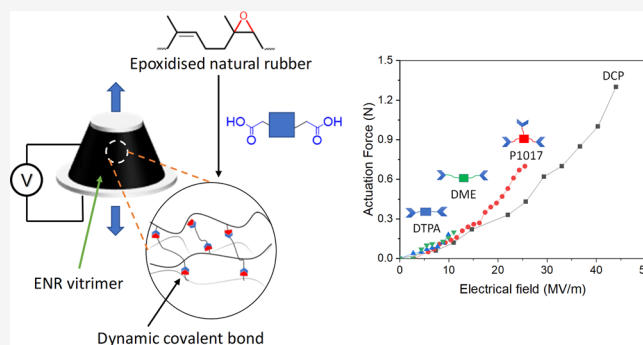


Article Recommendations



Supporting Information

**ABSTRACT:** The growing demand for smart polymeric transducers such as dielectric elastomer actuators and energy harvesters has urged the use of sustainable and recyclable elastomeric materials. Vitrimer chemistry has shed light on future reprocessable and recyclable thermosets and elastomers. In this work, epoxidized natural rubber (ENR) vitrimers were prepared using diacid or triacid cross-linkers and formed covalently cross-linking networks via thermally triggered reversible  $\beta$ -hydroxy ester bonds. The cross-linked ENR elastomers exhibited Arrhenius-type viscoelastic behavior with a complete stress relaxation between 140 and 160 °C, that is, vitrimer characteristics, which were highly dependent on the cross-linking temperature. The mechanical and dielectric properties of the ENR vitrimers can be tuned by varying the molecular structure and concentration of the cross-linkers. Among the diacid and triacid cross-linkers, Ripol 1017 fatty polyacid (P1017) and 3,3'-dithiopropionic acid (DTPA) had similar effects on the cross-linking density and mechanical properties of the ENR vitrimers. The highest tensile strength of  $8.70 \pm 1.9$  or  $15.6 \pm 2.6$  MPa was obtained at 6 mol % of P1017 or DTPA, respectively. While for diamide-based diacid cross-linker (DME), 8 mol % was needed to reach the highest tensile strength of  $13.1 \pm 2.7$  MPa for the elastomer. The three ENR vitrimers showed increased relative permittivity  $\epsilon' = 5\sim 7$  at 1 kHz while maintaining low dielectric losses compared to traditional dicumyl peroxide-cured ENR, with  $\epsilon' = 3.57$  at 1 kHz. With the optimized acidic cross-linker concentrations of P1017 at 6 mol %, DTPA at 6 mol %, and DME at 8 mol %, the ENR vitrimers exhibited improved actuation capabilities at lower electrical fields. Utilizing dynamic cross-linkers to tune the electromechanical properties of dielectric elastomers and the reversibly cross-linked polymer networks will open new opportunities for smart and sustainable dielectric elastomer devices.



## INTRODUCTION

Dielectric elastomers (DEs) are electroactive polymers that can deform upon local electrostatic forces induced by the electric field generated between the two electrodes. The energy transduction performance of DEs is intrinsically determined by the dielectric permittivity, electrical breakdown strength, and mechanical stretchability of the elastomers.<sup>1</sup> The current commercial elastomers such as silicone and VHB have low relative permittivity ( $\epsilon'$ , 2~4), showing limited energy transduction efficiency when used for actuators and energy generators.<sup>2</sup> In addition, commercial elastomers are often produced by covalently crosslinking or vulcanizing to form permanent covalent cross-linking networks for enhanced mechanical robustness and chemical resistivity. However, the permanent cross-linked elastomers raised further challenges in repairing, reprocessing, or recycling, which highly limit the sustainable applications of the DEs.

The introduction of dynamic covalent bonds to elastomers opens new opportunities for reprocessable and recyclable elastomers as the dynamic covalent cross-links can break and

reform via dissociative or associative exchange mechanisms, allowing the covalent adaptable network to rearrange its network topology. The associative polymer networks, also termed as vitrimers, maintain a constant cross-linking density during the exchange reactions, and their viscoelastic behavior follows an Arrhenius law upon heating.<sup>3,4</sup> So far, a variety of associative exchange mechanisms have been investigated for producing vitrimer materials, such as transesterification,<sup>5-7</sup> transalkylation,<sup>8-11</sup> disulfide metathesis,<sup>12-14</sup> and transamination<sup>15</sup> reactions.

Natural rubber (NR) has a high electrical breakdown strength ( $E_b$ ), a low elastic modulus, and excellent mechanical toughness.<sup>16,17</sup> The epoxidation of NR leads to the formation

**Received:** April 8, 2022

**Revised:** June 6, 2022

**Accepted:** June 7, 2022

of oxirane rings along the polymer backbone, increasing polarity and reactivity. The epoxy groups can be utilized to form cross-linking points in epoxidized NR (ENR) via epoxy-carboxylic acid reactions instead of using double carbon bonds via traditional radical curing agents.<sup>18</sup> The epoxy-carboxylic acid reaction generates  $\beta$ -hydroxy ester linkages, allowing the cross-linked ENR to undergo network rearrangement upon heating.<sup>4</sup> Different acidic cross-linkers were investigated for ENR, such as aliphatic carboxylic acid,<sup>19</sup> fatty acids,<sup>20</sup> and carboxylic group-functionalized fillers.<sup>21</sup> However, the formation of permanent cross-links due to self-polymerization of the remaining epoxy groups in ENR is unavoidable, as is the lack of free hydroxy groups to take part in the transesterification,<sup>4</sup> which hinders the full stress relaxation of the elastomer.<sup>22</sup> As a result, the mechanical properties of the vitrimer-like ENRs may change with recycling cycles.<sup>20</sup> This is undesirable for dielectric elastomeric device applications, as the self-healing or reprocessibility is compromised with the reliability of the elastomers.

The energy conversation performance of elastomers is highly dependent on the dielectric permittivity ( $\epsilon_r$ ), the electrical breakdown strength ( $E_b$ ), and Young's modulus ( $Y$ ); figure of merit (actuation) =  $3\epsilon_0\epsilon_r E_b^2/Y$  for actuation and for energy harvesting, and the figure of merit (generation) =  $\epsilon_0\epsilon_r E_b^{2.1}$ . From the figure of merits, the increase in relative permittivity and electrical breakdown strength and decrease in Young's modulus will improve the performance of the DE device. However, the polarity and mechanical properties of the elastomers are also affected by the selection of polar dynamic cross-linkers. Zhang et al. reported silicone rubber-based DE cross-linked via  $\beta$ -hydroxy ester exchangeable bonds,<sup>23</sup> but the effect of dynamic covalent bonds on the electromechanical properties of elastomeric vitrimers is yet to be studied.

In this work, three types of diacid cross-linkers with different chemical structures and polarities are studied for cross-linking of ENR via oxirane ring-opening reactions. The dynamic cross-links are composed of  $\beta$ -hydroxy ester linkages that enable network rearrangement at elevated temperatures. The effects of molecular structures and polarity of the cross-linkers on the electromechanical properties, viscoelasticity, and mechanical properties are investigated. The actuation performance of the resultant ENR vitrimer elastomers was demonstrated.

## EXPERIMENTAL SECTION

**Materials.** ENR (25%, ENR25) ( $M_n \approx 225,000$  g·mol<sup>-1</sup>) was purchased from Sanyo Trading Asia Co., Ltd. Japan. 1,2-Dimethylimidazole 97% (DMI), zinc acetylacetonate (Zn(acac)<sub>2</sub>), 3,3'-dithiopropionic acid (DPTA), dodecanedioic acid (DDCA), titanium(IV) isopropoxide (TIPP), and acetone were purchased from Sigma-Aldrich. Pripol 1017 was kindly provided by Croda. Carbon black grease was purchased from MG Chemicals. Jeffamine EDR-148 diamine was kindly provided by Huntsman.

**Synthesis of DDCA-Modified Jeffamine EDR-148 Diamine (DME).** For a typical synthesis, 24.18 g (0.1 mol, 2.1 equiv) of DDCA was added into a 250 mL round-bottom flask. The flask was purged by vacuum and nitrogen prior to being transferred into an oil bath and preheated to 130 °C. DDCA was left to melt completely under nitrogen for 30 min with gentle stirring. Then, 7.4 g (0.05 mol, 1 equiv) of Jeffamine EDR 148 was added dropwise into the flask. TIPP (10 wt %) was added, and the mixture was stirred for 1 h under nitrogen. A Dean–Stark apparatus was then fixed, and the

mixture was left to react under vacuum. After 5 h, the flask was cooled down to room temperature, and the solution turned into a solid after 5 min. The light brown solid product [denoted as diamide-based diacid cross-linker (DME)] was then ground and washed with 100 mL of acetone before drying under vacuum at 40 °C for 24 h, yield  $\approx$ 70%. <sup>1</sup>H NMR (400 MHz, DMSO-*d*<sub>6</sub>):  $\delta$  7.43 (br, 4H), 3.52 (br, 4H), 3.43 (br, 4H), 3.2 (br, 4H), 2.19 (t,  $J$  = 6.8 Hz, 4H), 2.09 (br, 4H), 1.52 (br, 8H), 1.40–1.20 (br, 24H).

**Elastomer Compounding.** ENR with different acid cross-linkers was compounded using a HAAKE PolyLab OS internal mixer. Briefly, ENR was first charged into the chamber at 50 °C for mastication. After 4 min, Pripol 1017, DMI as a curing catalyst, and Zn(acac)<sub>2</sub> as a transesterification catalyst were added gradually. The compound was mixed for 15 min at a rotor speed of 70 rpm. The samples are denoted as P1017  $x$  mol %, where  $x$  is the molar equivalent ratio of the carboxyl groups of the cross-linker and epoxy groups of ENR. The equimolar of DMI and Zn(acac)<sub>2</sub> are 200 and 10% relative to the carboxylic group of the cross-linkers, respectively. For ENR cross-linked with DPTA or DME, the same procedures were followed.

For the reference sample, ENR was first charged into the chamber at 50 °C for mastication. After 5 min, 1 phr of dicumyl peroxide (DCP) was added, and the compound was mixed for a total of 10 min at a rotor speed of 70 rpm. The mixed compounds were left to rest overnight prior to curing.

**Sample Preparation.** The curing characteristics of mixed compounds were evaluated using a MonTech Moving Die Rheometer following ISO 6502-1:2018. The oscillation angle of the moving die was 1° arc at a frequency of 1.77 Hz. The curing temperature was fixed at 150 °C to avoid side reactions. The curing characteristics at 150 °C of ENR mixed with DCP (a), P1017 (b), DTPA (c), and DME (d) are shown in Figure S1. A curing time of 60 min was selected for all samples cured with polyacids and 20 min for the control sample cured with DCP.

The curing took place in a Rondol manual hot press at 150 °C under 10 MPa. Sheets of 100 × 100 × 1 (mm) were prepared for tensile and stress-relaxation specimens. Thin films of 350  $\mu$ m thickness with a diameter of 15 cm were prepared for the measurement of dielectric properties and actuation performance.

**Characterization.** <sup>1</sup>H NMR was carried out in DMSO-*d*<sub>6</sub> using a Bruker Avance III HD 400 MHz spectrometer. The spectra were processed using an ACD/Labs NMR processor version 12.1. Fourier transform infrared (FT-IR) was carried out on Bruker Tensor 27 at a resolution of 2 cm<sup>-1</sup> with 64 scans to collect spectra of raw materials, uncured, and cured compounds.

The cross-link density of cured ENR samples was determined from the equilibrium swelling experiment. Samples were weighed ( $m_0$ ) and immersed in toluene at room temperature for 72 h, and the swollen samples were weighed ( $m_1$ ). Then, the samples were dried in vacuum at 60 °C until constant weight ( $m_2$ ). The swelling ratio was calculated via equation  $Q = m_1 - m_0/m_0$ , and the sol fraction was calculated via equation % sol =  $m_2 - m_0/m_0$ . The volume fraction of rubber ( $V_r$ ) was calculated via eq 1.

$$V_r = \frac{\frac{m_2}{\rho_r}}{\frac{m_2}{\rho_r} + \frac{(m_1 - m_2)}{\rho_s}} \quad (1)$$

in which  $p_r$  and  $p_s$  are the densities of the rubber and solvent, respectively (for ENR  $p_r = 0.96 \text{ g/cm}^3$  and toluene  $p_s = 0.865 \text{ g/cm}^3$ ). The cross-link density ( $\nu_e$ ) was then calculated using the Flory–Rehner equation<sup>24</sup>

$$\nu_e = \frac{-[\ln(1 + V_r) + V_r + \chi V_r^2]}{V_1 \left( V_r^{1/3} - \frac{V_r}{2} \right)} \quad (2)$$

where  $V_r$  is the molar volume of the solvent (for toluene,  $V_r = 106.3 \text{ cm}^3/\text{mol}$ ), and  $\chi$  is the interaction parameter between the rubber and solvent (for toluene  $\chi = 0.39$ ).

Tensile testing was conducted using a Shimadzu Autograph AGS-X tensile tester according to ASTM-D638 at room temperature. The specimens (thickness  $\approx 1 \text{ mm}$ , width  $\approx 3.18 \text{ mm}$ , and gauge length  $\approx 7.62$ ) prepared with the ASTM-D638 V-type die were tested with a cross-head speed of 500 mm/min and a 10 kN load cell. The cyclic stress softening test was conducted by stretching the specimens to 200, 400, and 600% strains and back to 0% strain under a controlled extension rate of 100 mm/min.

The stress relaxation of cured compounds was evaluated using DMA in the tension mode. Rectangular specimens of  $15 \times 5 \times 1 \text{ (mm)}$  were cut from the  $100 \times 100 \times 1$ . The sample was subjected to a constant strain of 3% under isothermal conditions, and the stress decay was measured over time.

Dielectric properties of cured samples were characterized by impedance spectroscopy using a Princeton Applied Research Parastat MC with a PMC-2000 card between 1 Hz and 1 MHz with an applied voltage of 1 V.

The setup for a cone-shape actuation test is shown in Figure 1. The ENR elastomer film ( $\sim 350 \mu\text{m}$  in thickness) was

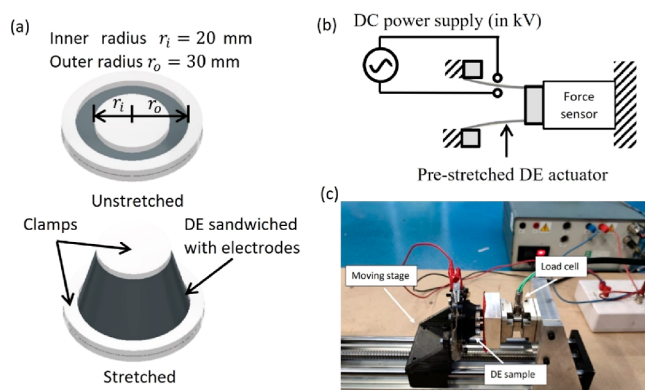


**Figure 1.** (a) Configuration of the cone-shaped DE actuator, (b) schematic diagram of the DE actuation tests, and (c) actual setup for DE actuation.

clamped with two sets of rigid frames. Electrodes (carbon black grease) were applied to the film to form a circular electrode region with an inner radius of  $r_i = 20 \text{ mm}$  and an outer radius of  $r_o = 30 \text{ mm}$ . The sample is attached to the moving stage at one end and to the load cell (from Kistler) at the other end. The load cell measures the force changes on the sample for calculating the actuation force output. The elastomer structure was pre-stretched with a stroke of 20 mm in the direction of thickness using a linear stage driven using a stepper motor. The

inner ring frame was fixed on a sensor that takes force measurements; the outer ring frame was fixed on the stage with conductive foil wrapped on the edge for connecting to the high-voltage power source.

The actuation force is defined as the net force between two stages of the device, i.e., with and without activation. The driving voltage was applied in steps, increasing from 0 kV to the point when the electrical breakdown occurs. At each driving voltage  $V_A$ , the corresponding electrical field  $E_A$  was calculated as  $E_A = V_A/h\lambda_A$ , where  $h$  is the thickness of the stretched DE film and  $\lambda_A$  is the areal stretch of the electrode region that can be estimated as a function of the stroke of the moving stage,  $l$ , as (i.e.  $\lambda_A = 2.2$  at  $l = 20 \text{ mm}$ )

$$\lambda_A = \frac{(\pi r_o + \pi r_i) \sqrt{(r_o - r_i)^2 + l^2}}{(r_o^2 - r_i^2)\pi}$$

Note that this equation only estimates the overall deformation of the electrode region. The actual deformation is inhomogeneous, and a more accurate estimation requires a sophisticated material model.<sup>25</sup>

The calculated electrical field at electrical breakdown using the above equations would be lower than the actual value. Therefore, it can be counted as a conservative approximation of electrical breakdown strength. In the actuation test, stress relaxation was found to be significant in pre-stretching the samples (i.e., strain over 200%) and negligible in actuation (i.e., strain below 20%). To mitigate any effect of stress relaxation, pre-stretched samples were left for a long period of time (i.e., for over half an hour) to ensure that the relaxation process had settled before any experiments.

## RESULTS AND DISCUSSION

To obtain dielectric ENR vitrimers, three carboxylic acid-containing cross-linkers with different molecular structures and polarities are investigated. As shown in Figure 2a, the P1017 is a biosourced fatty acid mixture with a bulky structure, DTPA is a diacid of short aliphatic structure with a disulfide linkage (Figure 2b),<sup>12</sup> and the DME synthesized in this work contains a long flexible aliphatic chain (Figure 2c). The reaction between the diacids and epoxy groups of ENR leads to a covalently cross-linked network via  $\beta$ -hydroxy ester bonds, which are reversible via associative exchange reactions at elevated temperatures (Figure 2d). The DCP cross-linked ENR elastomer was prepared as a control.

First, the diacid DME cross-linker was synthesized by the addition reaction of Jeffamine EDR 148 with DDCA, following a procedure described in the Experimental Section. The molar ratio between DDCA and EDR was set as 2.1/1 to restrict the potential polymerization reaction. The carboxylic group of DDCA reacts with the primary amine of EDR to form a secondary amide. After the reaction, a dimeric acid named DME was formed. As characterized by <sup>1</sup>H NMR shown in Figure 3a, the DME cross-linker showed signals from the methylene groups on DDCA at 2.19 (a), 1.52 (b), 1.27 (c), and 2.09 (d) ppm. The signals at 3.52 (g), 3.43 (h), and 3.21 (f) ppm were assigned to the methylene groups of DME. The characteristic peak at 7.43 ppm represents the chemical shift of the C(O)–NH– proton. The relative intensity ratio of peaks (b,h) is 8.01/3.95, suggesting the molar ratio of DDCA/EDR of approximately 2/1, which is consistent with that of the structure of DME given in Figure 3a.

The cross-linking efficiency of different cross-linkers was evaluated by measuring the cross-linking density of the cured ENR samples using equilibrium swelling experiments, where

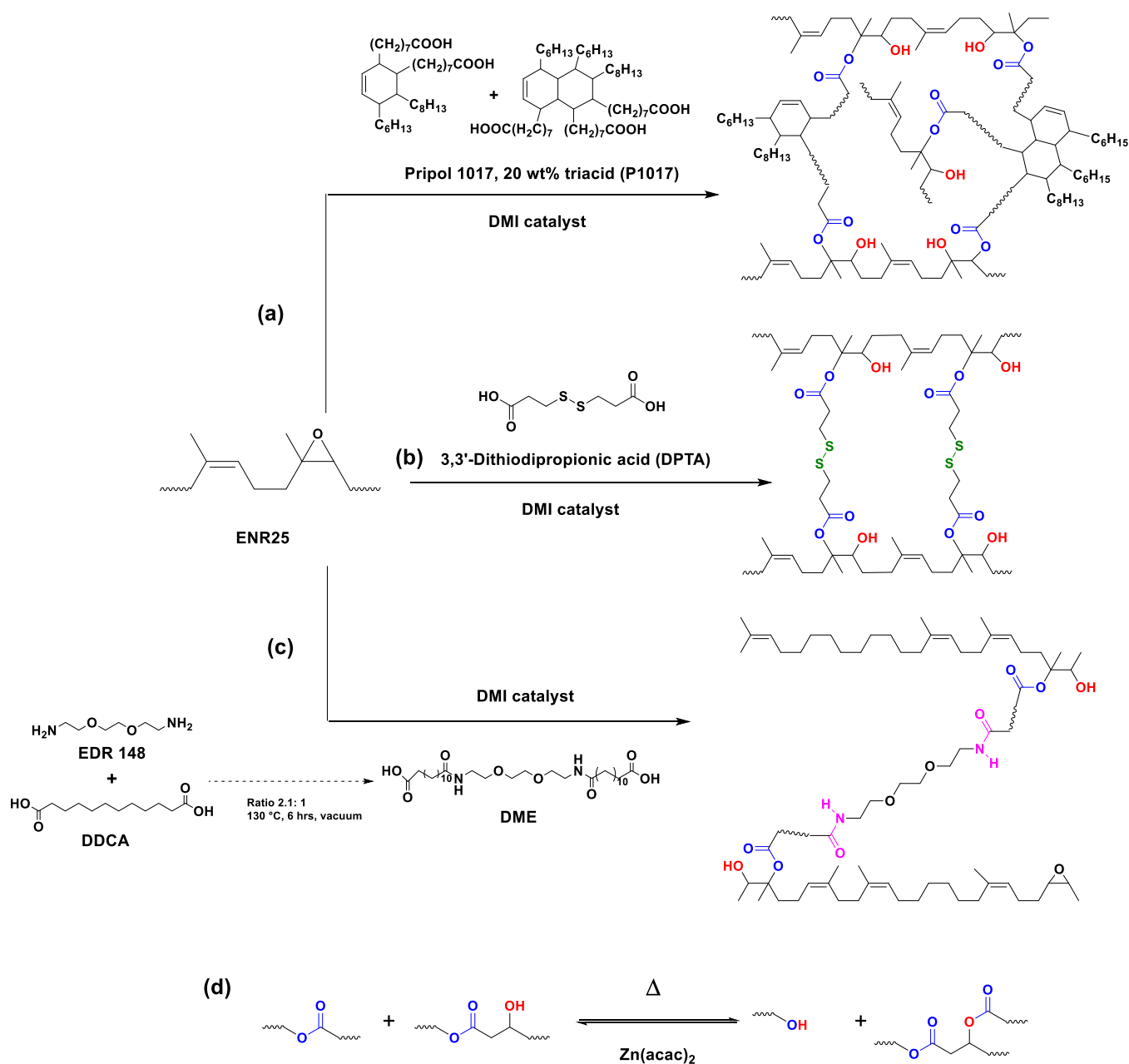


**Figure 2.** Schematic of cross-linking reactions of ENR using three different cross-linkers: (a) P1017, (b) DTPA, and (c) DME; and (d) dynamic exchange mechanism of transesterification.

the swelling ratio, cross-link density, and sol fraction were quantified. The results are reported in Table S1. The control sample shows a swelling ratio of 8.2 and a soluble fraction of 9 wt %, indicating a loosely cross-linked network and reflecting a low cross-link density of  $3.63 \times 10^{-5}$  mol/cm<sup>3</sup>. The soluble fraction, corresponding to the content of uncross-linked materials, remains low between 4 and 9 wt %, except for 4 mol % DME cross-linked ENR, which reaches 14 wt % of extractable content. The cross-link densities of cured ENR/P1017 and ENR/DTPA are similar and higher than those of ENR/DME at all loadings. The difference in the cross-link density between samples is in good agreement with the curing curves in Figure S1. The torque nearly reached a plateau after 60 min in the case of ENR/P1017 and ENR/DTPA, while the torque value of ENR/DME samples increased much more slowly over 60 min. This indicates that the chemical structures

of the carboxylic acid-based cross-linkers have an effect on the cross-linking reactions and should be carefully selected for effective network formation.

As characterized by FT-IR (Figure 3b–d), the original ENR shows absorption bands at 1261 and 873 cm<sup>-1</sup>, respectively, related to asymmetric and symmetric stretching of epoxy groups on the ENR backbone. During the curing process, the epoxy group reacts with carboxylic acid at elevated temperatures and forms  $\beta$ -hydroxy ester bonds. This reaction then gives rise to signals related to hydroxy esters. The diacid- or triacid-cured samples all showed new absorption bands at 3442 cm<sup>-1</sup> (broad O–H stretch), 1732 cm<sup>-1</sup> (C=O ester stretch), 1344 cm<sup>-1</sup> (O–H out of plane bend), and 1117 cm<sup>-1</sup> (C–O secondary alcohol stretch), confirming the epoxy ring-opening reaction and the formation of  $\beta$ -hydroxy esters. This observation indicates that the curing occurred under the

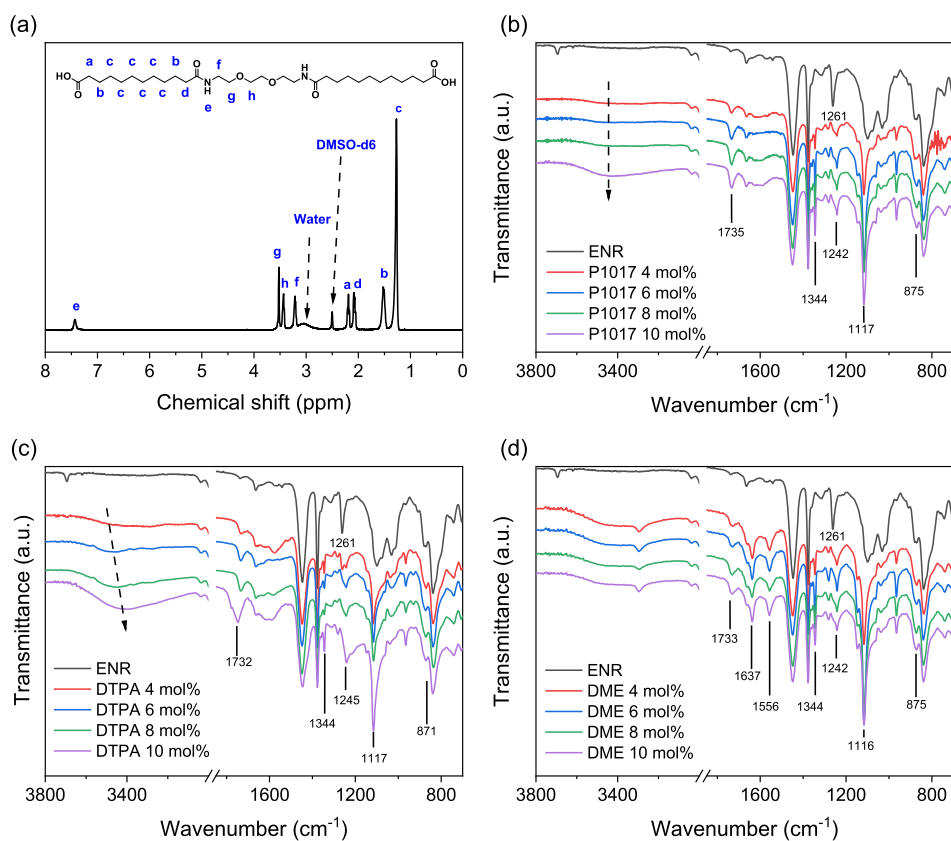


Figure 3. (a) <sup>1</sup>H NMR spectrum of DME; FT-IR spectra of ENR cured with different proportions of P1017 (b), DTPA (c), and DME (d).

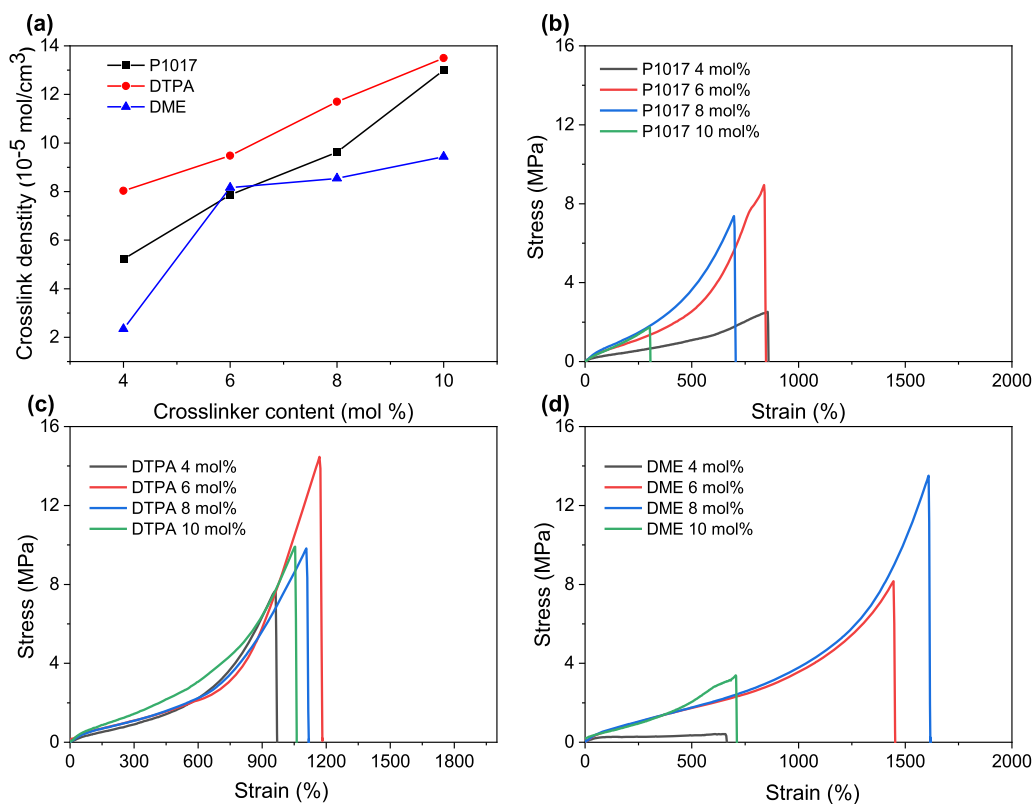
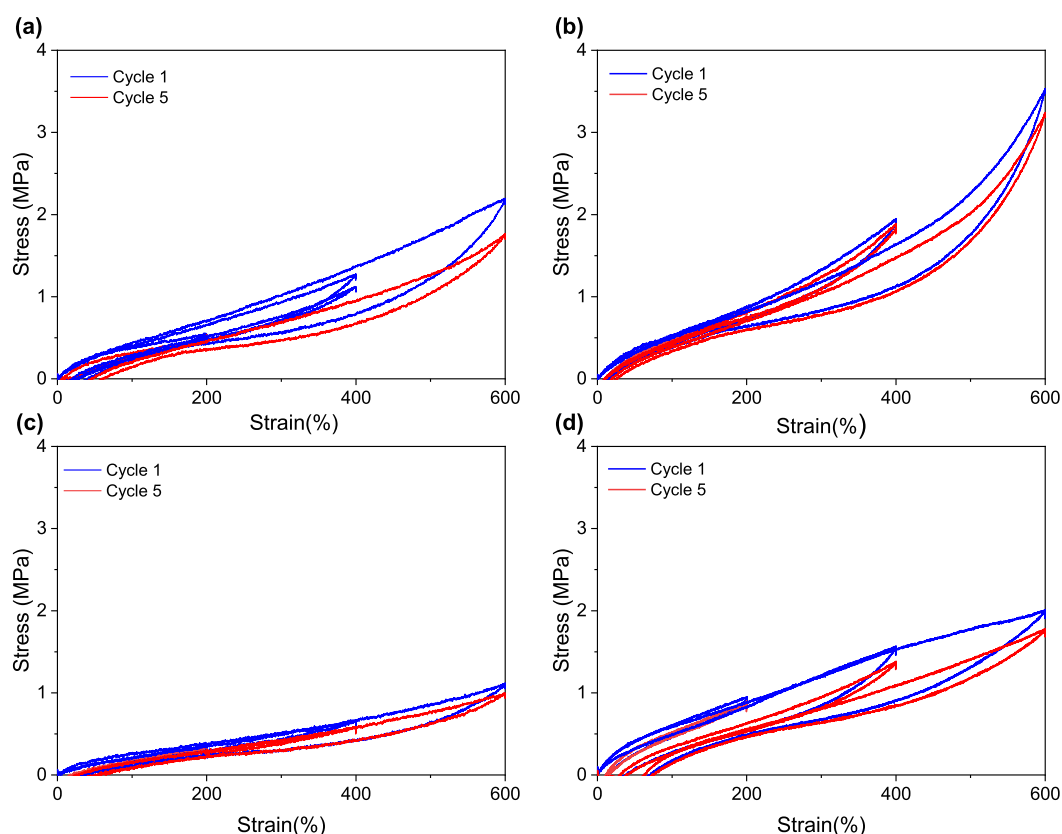


Figure 4. (a) Cross-link density and stress–strain results of ENR samples cross-linked with (b) P1017, (c) DTPA, and (d) DME.

exact reaction mechanism. With the increase in the cross-linker concentration, the peak intensity at 1732 cm<sup>-1</sup> (C=O ester

stretch), 1344 cm<sup>-1</sup> (O–H bend), and 1117 cm<sup>-1</sup> (C–O stretch) was increased in all cases. Also, the absorption band at



**Figure 5.** Cycling stress–strain testing of ENR samples cured with (a) DCP 1 phr, (b) P1017 6 mol %, (c) DTPA 6 mol %, and (d) DME 8 mol %.

1261  $\text{cm}^{-1}$  (asymmetric epoxy stretch) shifted to 1241~1245  $\text{cm}^{-1}$  with an intensity increase after cross-linking. The peak shift is possibly due to the hydrogen bonding formation between epoxy or carbonyl with hydroxyl within the network.<sup>20</sup> The broad bands at 3485~3441  $\text{cm}^{-1}$  (O–H stretching) are observed in all spectra. However, the change in intensity and shift of this broadband due to the increase in cross-linker concentrations are unclear. In the IR spectrum of cured ENR/DME, the secondary amide on DME was also observed from the absorption bands at 3294  $\text{cm}^{-1}$  (N–H stretch, secondary amide), 1637  $\text{cm}^{-1}$  (C=O stretching), and at 1560  $\text{cm}^{-1}$  (N–H in-plane bend), see Figure 3d.

Mechanical properties of DEs are crucial for ensuring stable actuation performance, which ideally requires high elongation ( $\epsilon > 200\%$ ), low elastic modulus ( $Y \approx 1$  MPa), and high tensile strength ( $\sigma > 2$  MPa) for continuous operation.<sup>1,17</sup> The cured ENR/DCP samples were tested to have tensile properties of  $\sigma = 1.63 \pm 0.4$  MPa,  $\epsilon = 530 \pm 100\%$ , and  $Y = 1.25 \pm 0.1$  MPa. For the diacid or triacid cross-linked ENRs, as shown in Figure 4b–d, the tensile properties of ENR/P1017 (4 mol %) were close to those of the cured ENR/DCP. As the P1017 content increased, both tensile strength and elongation at break increased to maximum values at 6 mol % ( $\sigma = 8.7 \pm 1.9$  MPa and  $\epsilon = 810 \pm 70\%$ ). A similar trend was observed in ENR/DTPA (6 mol %) with maximum tensile strength and elongation at breaks of  $15.6 \pm 2.6$  MPa and  $1320 \pm 130\%$ , respectively. The ENR/P1017 samples are generally weaker than ENR/DTPA samples, which may be due to their bulky structure that hinders the chain mobility and results in a lower cross-linking density over different concentrations, as shown in Figure 4a. The cured ENR/DME at 4 mol % shows poor tensile strength with a lower cross-link density since the polar

structure of DME possibly hinders chain diffusion. However, these secondary amides can form hydrogen bonds with carbonyl groups or unreacted oxiranes on the ENR structure, reinforcing the tensile properties of cured ENR. Thus, the tensile strength and elongation of cured ENR/DME increase gradually at 6–8 mol % until the network is over-cross-linked at 10 mol % despite the slight increase in cross-link density.<sup>26,27</sup> The stress at 100% strain (M100) of the acid-cured ENR increased slightly from 0.2~0.3 MPa at 4 mol % to around 0.5~0.6 MPa at 6–10 mol %. The cured ENR with 6 mol % P1017, 6 mol % DTPA, and 8 mol % DME were selected for further investigation, given their balanced strength and stretchability.

In addition, the hysteresis of cured ENRs affects the input voltage and output displacement of the actuation performance of the DEs, thus challenging the precise control and stability. The hysteresis behavior of the ENR samples was characterized by cyclic stress–strain testing at room temperature. As shown in Figures 5 and S3, at 400% strain, the ENR samples cured with 6 mol % of P1017 and DTPA and 8 mol % of DME showed hysteresis losses of 10.5, 22.9, and 22.8%, respectively. In comparison, the ENR cured with 1 phr DCP showed a hysteresis loss of 30.4%. Similarly, at the strain of 600%, the hysteresis losses of the samples were increased to 15, 30.3, and 37.3%, respectively, and the DCP-cured ENR showed 35.5% hysteresis. The three types of acidic cross-linker-cured ENRs have higher cross-linking densities than the DCP-cured ENR (see Table S1), which may constrain the polymer chain movement, lowering the energy loss. The DME-cured samples showed the largest residue strain and hysteresis area at 200 and 400% strain due to their lower cross-link density. The lower hystereses of ENR/P1017 and ENR/DTPA are favorable for

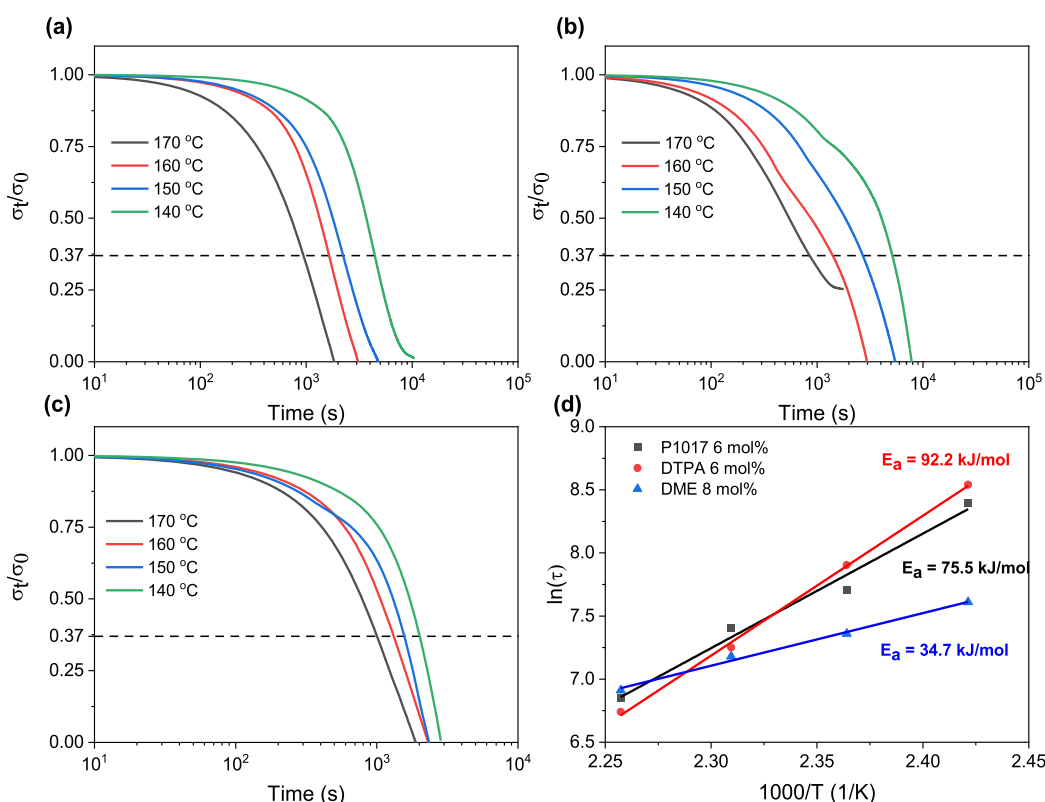


**Figure 6.** Isothermal stress relaxation of (a) P1017 6 mol %, (b) DTPA 6 mol %, and (c) DME 8 mol %; and (d) Arrhenius plot.

actuation application because they help maintain the performance over cycles.

The stress relaxation behavior can evaluate the dynamic nature of the cross-linked polymer networks. Figure 6a–c showed that the three types of polyacid-cured elastomers could relax 100% of their initial stress at elevated temperatures (140–170 °C) under isothermal conditions, except for DTPA of the 6 mol % sample at 170 °C. The complete stress relaxation indicates typical vitrimer characteristics of the polyacid-cured ENRs. While vitrimer-like properties of diacid-cured ENR were reported in a previous study, their stress-relaxation was only partially recovered.<sup>4</sup> This may be due to their higher curing temperature at 180 °C for 45 min<sup>4,20</sup> that causes side cross-linking reactions. In this study, the curing conditions were kept at 150 °C for 60 min to promote  $\beta$ -hydroxy ester bond formation over permanent covalent bond formation from epoxide ring opening.<sup>28,29</sup> The stress reduction of the samples was recorded under a constant strain isothermally.

The stress relaxation time ( $\tau^*$ ) is the amount of time required for the stress to reduce to 37% ( $1/e$ ) of the initial value. The time required for self-healing or reprocessing of the material can be estimated from the value of  $\tau^*$ .<sup>12</sup> For elastomeric vitrimers that are covalently cross-linked with dynamic associative bonds, the bond exchange and network rearrangements are temperature dependent. The time constant decreases when increasing the temperature for all the vitrimer samples. As the temperature increases from 140 to 170 °C, the value of  $\tau^*$  decreases significantly from 4350 to 645 s for ENR/DTPA 6 mol %, from 4400 to 940 s for ENR/P1017 6 mol %, and moderately from 2020 to 1025 s for ENR/DME 8 mol %. Therefore, a higher temperature facilitates the bond exchange, thus lowering  $\tau^*$ . When plotting the  $\ln(\tau^*)$  as a

function of  $1000/T$  for the polyacid-cured elastomers (Figure 6d), a linear behavior is observed, indicating that the  $\tau^*$  follows the Arrhenius law, confirming that the polyacid-cross-linked ENRs exhibit vitrimer characteristics. Also, there is no significant change in the cross-link density for all samples after stress relaxation at 150 °C, see Figure S6. Thus, the associative exchange occurs without significant loss of network integrity, and no significant post-curing occurs.

The activation energy for the network rearrangement can be calculated from the linear fitting curve of  $\tau^*$  from Figure 6d via the Arrhenius equation,  $\ln(\tau) = E_a/RT + \ln A$ , where  $E_a$  is the activation energy of the viscous flow,  $R$  is the gas constant,  $T$  is the absolute temperature, and  $A$  is a pre-exponential factor. ENR/P1017 6 mol % and ENR/DTPA 6 mol % showed  $E_a = 75.5$  and 92 kJ/mol, respectively, within the range of transesterification reaction (80–120 kJ/mol) as reported in the literature.<sup>20,30</sup> It should be noted that the DTPA can also undergo disulfide metathesis as a second bond-exchange mechanism at elevated temperatures. This can also be reflected in the stress relaxation curves, where DTPA displays two slightly decaying processes during viscous flow. In addition, disulfide tends to generate thiol radicals at high temperatures that are prone to react with the carbon–carbon double bonds of the ENR to form permanent cross-links. This reaction might have occurred in ENR/DTPA at 170 °C, which fully hindered its stress relaxation (Figure 5b). Finally, the ENR/DME 8 mol % had the lowest  $E_a = 34.7$  kJ/mol, which the presence of hydrogen bonding may explain. Indeed, the DME possesses two secondary amides and the hydroxyl group generated from the epoxy-carboxylic acid reaction. These groups can form hydrogen bonds and positively charge the carbonyl group of esters. The charge increases the electrophilicity of carbonyl, increasing its reactivity toward nucleophilic attack. The

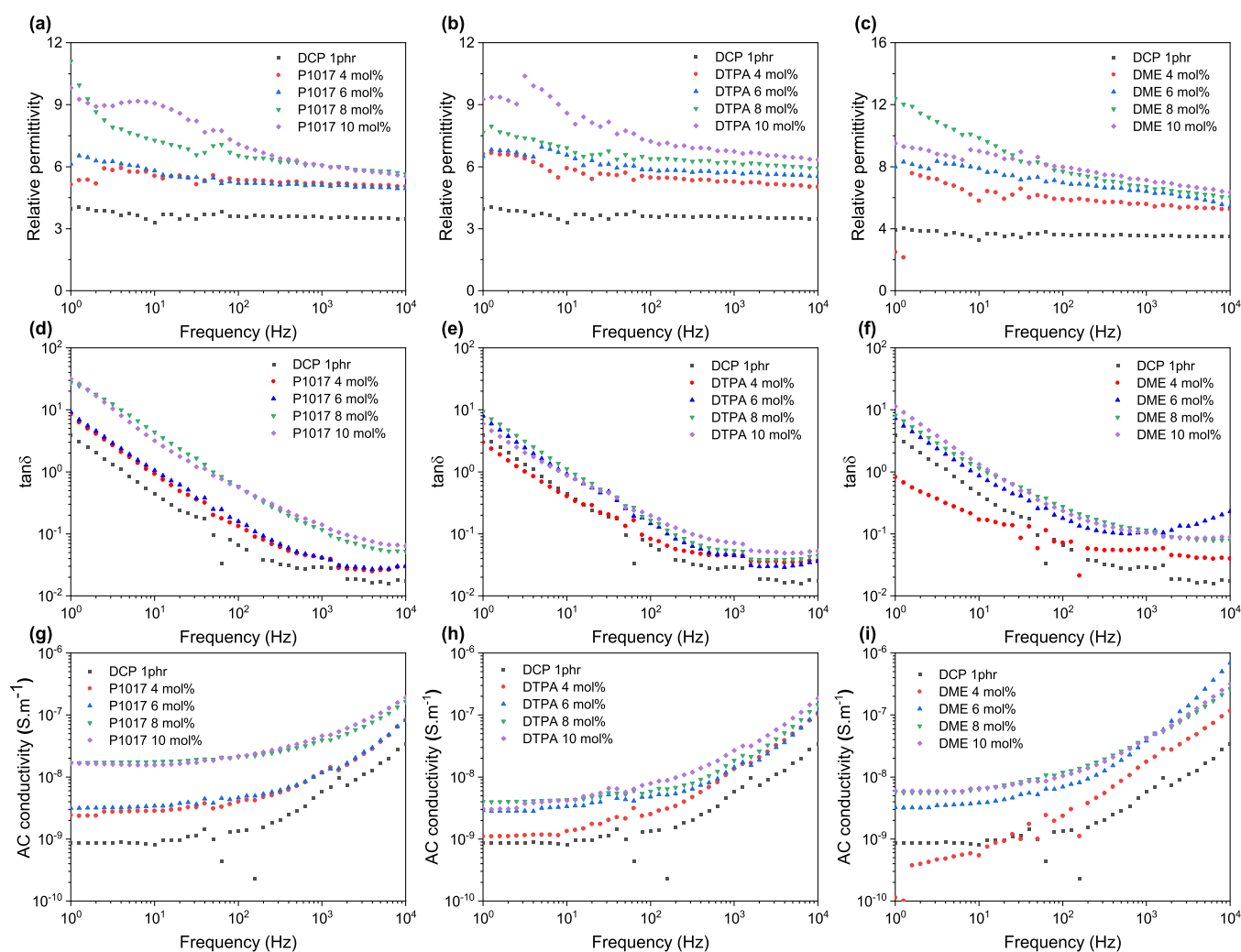


**Figure 7.** Frequency dependence of relative permittivity (a–c), dielectric loss tangent ( $\tan \delta$ ) (d–f), and AC conductivity (g–i) of ENR cured by P1017, DTPA, and DME at different concentrations.

hydrogen bonding thus accelerates the transesterification.<sup>31,32</sup> As a result, the ENR/DME samples exhibit faster network rearrangement with a lower  $E_a$  of 34.7 kJ/mol.

The effects of the three acidic cross-linkers on the dielectric properties of cross-linked ENR are examined. As shown in Figure 7 and Table S2, the introduction of polar cross-linkers increased the relative permittivity of the elastomer, which might be due to the generated polar hydroxyl groups during the curing process.<sup>33</sup> In addition, the relative permittivity  $\epsilon'$  of the elastomers was increased with the cross-linker loading. For ENR/P1017, the  $\epsilon'$  at 1 kHz is increased from 3.57 to 6.07 when the P1017 content is increased to 10 mol %. Similarly, the  $\epsilon'$  at 1 kHz of ENR/DTPA is increased from 5.28 to 6.75 as the content of diacids is increased from 4 to 10 mol %. At the same time, the ENR/DME samples showed a higher  $\epsilon'$  increase from 5.59 to 7.14. The polyacid cross-linked ENR elastomers showed higher relative permittivity than the DCP-cured ENR while maintaining low losses ( $\tan \delta < 0.1$ ). The phase angle of  $90^\circ$  and AC conductivity of magnitude of  $10^{-8}$  at 1 kHz confirm the insulating nature of all the cured samples. The enhancing dielectric properties of ENR through the acidic cross-linkers is a facial approach as compared to traditional methods, such as modifying NR with 50 phr of BaTiO<sub>3</sub> and 30 phr of dioctyl phthalate, which only showed  $\epsilon' = 4.03$  at 1

kHz.<sup>34</sup> Together with the enhanced mechanical strength and elongation, the polyacid cross-linked ENRs are promising for high-performance DEs and actuation applications. The ENR/P1017 (6 mol %), ENR/DTPA (6 mol %), and ENR/DME (8 mol %) were further tested for actuation due to their balanced electromechanical properties.

The actuation results of different ENR-actuators are compared in Figure 8. The DCP-cured ENR-based actuator generated a maximum actuation force of 1.3 N at 44 MV/m and failed at 48 MV/m due to electrical breakdown. In comparison, cured ENR/acidic cross-linkers exhibited improved actuation capabilities at lower electrical fields at the cost of electrical breakdown strength. At around 10 MV/m, the ENR/DTPA 6 mol % and the ENR/DME 8 mol %-based actuators generated a force output of 0.18 N, which was 50% higher than that of 0.12 N from the DCP-based actuator. At 35 MV/m, the ENR/P1017-6 mol %-based actuator generated a force of 0.7 N, which was over 60% higher than that of 0.43 N from the DCP-cured ENR-based actuator. Figure 8 also showed that the diacid-cured elastomer-based actuators would require lower driving voltages than the ENR/DCP-based actuator to generate the same actuation force. For example, to generate an actuation force of 0.7 N, the operating electrical field of ENR/P1017-6 mol % is over 20% lower than that of



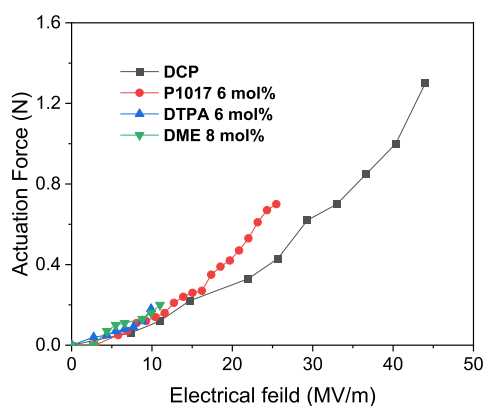


**Figure 8.** Actuation performance of the ENR elastomer cross-linked with DCP 1phr, 6 mol % P1017, 6 mol % DTPA, or 8 mol % DME.

ENR/DCP (i.e., 26.63 MV/m compared with 35 MV/m). Such an enhancement in material properties would benefit the development of DE devices for low-voltage-driven applications.

## CONCLUSIONS

ENR-based DE vitrimers were synthesized using diacid or triacid cross-linkers (P1017, DTPA, or DME). The molecular structures and concentrations of the carboxylic acid-containing cross-linkers are investigated by evaluating their reactivity, cross-linking density, mechanical properties, and dielectric properties of the polymer networks and compared with traditional peroxide (DCP)-cured ENR as a control. The resultant associative  $\beta$ -hydroxy ester bonds enabled complete stress relaxation and Arrhenius viscoelastic behavior of ENR/P1017 and ENR/DME between 140 and 170 °C. The ENR vitrimers exhibited a generally high tensile strength (8.7~15.6 MPa) and elongation at break (750~1600%) while maintaining a low modulus ( $Y < 1.5$  MPa). The polarity of DME containing a secondary amide restricts its dispersion in the ENR matrix, resulting in lower cross-linking efficiency. Both P1017 and DTPA cross-linked ENR exhibited high tensile strength and elasticity for DE applications. In view of vitrimer formation, the curing under a lower temperature was proven adequate to avoid side reactions. In addition, the acidic cross-linkers increased the relative permittivity of the ENR vitrimers ( $\epsilon' = 5\sim 7$  at 1 kHz) while maintaining low dielectric losses, thus allowing the ENR vitrimer-based actuators to be more responsive to low voltage than DCP-cured ENR-based ones.

## ASSOCIATED CONTENT

### Supporting Information

The Supporting Information is available free of charge at <https://pubs.acs.org/doi/10.1021/acs.iecr.2c01229>.

Details on characteristic curing curves, cross-link density, solid content, mechanical properties, hysteresis loss, dielectric properties of cured ENR, and temperature-dependent FT-IR analysis of cured ENR/P1017 at 8 mol % (PDF)

## AUTHOR INFORMATION

### Corresponding Author

Chaoying Wan – International Institute for Nanocomposites Manufacturing (IINM), WMG, University of Warwick, CV4 7AL Coventry, U.K.; [orcid.org/0000-0002-1079-5885](https://orcid.org/0000-0002-1079-5885); Email: [chaoying.wan@warwick.ac.uk](mailto:chaoying.wan@warwick.ac.uk)

## Authors

**Khoa Bui** – International Institute for Nanocomposites Manufacturing (IINM), WMG, University of Warwick, CV4 7AL Coventry, U.K.; CY Cergy-Paris Université, 95000 CERGY, France; [orcid.org/0000-0002-1256-7544](https://orcid.org/0000-0002-1256-7544)  
**Alan M. Wemys** – International Institute for Nanocomposites Manufacturing (IINM), WMG, University of Warwick, CV4 7AL Coventry, U.K.; [orcid.org/0000-0002-5919-9881](https://orcid.org/0000-0002-5919-9881)  
**Runan Zhang** – Department of Mechanical Engineering, University of Bath, BA2 7AY Bath, U.K.  
**Giao T. M. Nguyen** – CY Cergy-Paris Université, 95000 CERGY, France  
**Cedric Vancaeyzeele** – CY Cergy-Paris Université, 95000 CERGY, France; [orcid.org/0000-0002-9748-1562](https://orcid.org/0000-0002-9748-1562)  
**Frederic Vidal** – CY Cergy-Paris Université, 95000 CERGY, France; [orcid.org/0000-0001-9803-0918](https://orcid.org/0000-0001-9803-0918)  
**Cedric Plesse** – CY Cergy-Paris Université, 95000 CERGY, France

Complete contact information is available at:

<https://pubs.acs.org/10.1021/acs.iecr.2c01229>

## Notes

The authors declare no competing financial interest.

## ACKNOWLEDGMENTS

K.B. would like to acknowledge the Co-tutelle PhD program supported by EUTOPIA Alliance, project number PSI-AAP2019-000000073. K.B. would like to thank Miss Xiao Hu for moving die rheology experiments.

## REFERENCES

- (1) Ellingford, C.; Bowen, C.; McNally, T.; Wan, C. Intrinsically Tuning the Electromechanical Properties of Elastomeric Dielectrics: A Chemistry Perspective. *Macromol. Rapid Commun.* **2018**, *39*, No. e1800340.
- (2) Banet, P.; Zeggai, N.; Chavanne, J.; Nguyen, G. T. M.; Chikh, L.; Plesse, C.; Almanza, M.; Martinez, T.; Civet, Y.; Perriard, Y.; Fichet, O. Evaluation of dielectric elastomers to develop materials suitable for actuation. *Soft Matter* **2021**, *17*, 10786–10805.
- (3) Montarnal, D.; Capelot, M.; Tournilhac, F.; Leibler, L. Silica-like malleable materials from permanent organic networks. *Science* **2011**, *334*, 965–968.
- (4) Imbernon, L.; Norvez, S.; Leibler, L. Stress Relaxation and Self-Adhesion of Rubbers with Exchangeable Links. *Macromolecules* **2016**, *49*, 2172–2178.
- (5) Capelot, M.; Montarnal, D.; Tournilhac, F.; Leibler, L. Metal-catalyzed transesterification for healing and assembling of thermosets. *J. Am. Chem. Soc.* **2012**, *134*, 7664–7667.
- (6) Altuna, F. I.; Hoppe, C. E.; Williams, R. J. J. Epoxy Vitrimers: The Effect of Transesterification Reactions on the Network Structure. *Polymers* **2018**, *10*, 43.
- (7) Niu, X.; Wang, F.; Li, X.; Zhang, R.; Wu, Q.; Sun, P. Using Zn<sup>2+</sup>-Ionomer To Catalyze Transesterification Reaction in Epoxy Vitrimer. *Ind. Eng. Chem. Res.* **2019**, *58*, 5698–5706.
- (8) Obadia, M. M.; Mudraboyina, B. P.; Serghei, A.; Montarnal, D.; Drockenmuller, E. Reprocessing and Recycling of Highly Cross-linked Ion-Conducting Networks through Transalkylation Exchanges of C-N Bonds. *J. Am. Chem. Soc.* **2015**, *137*, 6078–6083.
- (9) Hendriks, B.; Waelkens, J.; Winne, J. M.; Du Prez, F. E. Poly(thioether) Vitrimers via Transalkylation of Trialkylsulfonium Salts. *ACS Macro Lett.* **2017**, *6*, 930–934.
- (10) Huang, J.; Zhang, L.; Tang, Z.; Wu, S.; Guo, B. Reprocessable and robust cross-linked elastomers via interfacial C N transalkylation of pyridinium. *Compos. Sci. Technol.* **2018**, *168*, 320–326.

- (11) Xu, W. Z.; Yu, W. W.; Chen, X.; Liao, S.; Luo, M. C. Based on transalkylation reaction the rearrangeable conventional sulfur network facile design for vulcanised diolefin elastomers. *J. Appl. Polym. Sci.* **2021**, *138*, 51182.
- (12) Imbernon, L.; Oikonomou, E. K.; Norvez, S.; Leibler, L. Chemically cross-linked yet reprocessable epoxidized natural rubber via thermo-activated disulfide rearrangements. *Polym. Chem.* **2015**, *6*, 4271–4278.
- (13) Ghorai, S.; Bhunia, S.; Roy, M.; De, D. Mechanochemical devulcanisation of natural rubber vulcanizate by dual function disulfide chemicals. *Polym. Degrad. Stab.* **2016**, *129*, 34–46.
- (14) Hernández, M.; Grande, A. M.; Dierkes, W.; Bijleveld, J.; van der Zwaag, S.; García, S. J. Turning Vulcanized Natural Rubber into a Self-Healing Polymer: Effect of the Disulfide/Polysulfide Ratio. *ACS Sustain. Chem. Eng.* **2016**, *4*, 5776–5784.
- (15) Denissen, W.; Rivero, G.; Nicolaÿ, R.; Leibler, L.; Winne, J. M.; Du Prez, F. E. Vinylogous Urethane Vitrimers. *Adv. Funct. Mater.* **2015**, *25*, 2451–2457.
- (16) Yang, D.; Xu, Y. J.; Ruan, M. N.; Xiao, Z. X.; Guo, W. L.; Wang, H. M.; Zhang, L. Q. Improved electric energy density and conversion efficiency of natural rubber composites as dielectric elastomer generators. *AIP Adv.* **2019**, *9*, 025035.
- (17) Madsen, F. B.; Daugaard, A. E.; Hvilsted, S.; Skov, A. L. The Current State of Silicone-Based Dielectric Elastomer Transducers. *Macromol. Rapid Commun.* **2016**, *37*, 378–413.
- (18) Pire, M.; Norvez, S.; Iliopoulos, I.; Le Rossignol, B.; Leibler, L. Imidazole-promoted acceleration of cross-linking in epoxidized natural rubber/dicarboxylic acid blends. *Polymer* **2011**, *52*, 5243–5249.
- (19) Algaily, B.; Kaewsakul, W.; Sarkawi, S. S.; Kalkornsurapranee, E. Enabling reprocessability of ENR-based vulcanisates by thermochemically exchangeable ester cross-links. *Plast., Rubber Compos.* **2021**, *50*, 315–328.
- (20) Salaeh, S.; Das, A.; Wiessner, S.; Stapor, M. Vitriimer-like material based on a biorenewable elastomer cross-linked with a dimeric fatty acid. *Eur. Polym. J.* **2021**, *151*, 110452.
- (21) Xu, C.; Cui, R.; Fu, L.; Lin, B. Recyclable and heat-healable epoxidized natural rubber/bentonite composites. *Compos. Sci. Technol.* **2018**, *167*, 421–430.
- (22) Wemyss, A. M.; Bowen, C.; Plesse, C.; Vancaeyzeele, C.; Nguyen, G. T. M.; Vidal, F.; Wan, C. Y. Dynamic cross-linked rubbers for a green future: A material perspective. *Mater. Sci. Eng. R Rep.* **2020**, *141*, 100561.
- (23) Liu, X. Y.; Sun, H. B.; Liu, S. T.; Jiang, Y. J.; Yu, B.; Ning, N. Y.; Tian, M.; Zhang, L. Q. Mechanical, dielectric and actuated properties of carboxyl grafted silicone elastomer composites containing epoxy-functionalized TiO<sub>2</sub> filler. *Chem. Eng. J.* **2020**, *393*, 124791.
- (24) Flory, P. J.; Rehner, J. Statistical Mechanics of Cross-Linked Polymer Networks II. Swelling. *J. Chem. Phys.* **1943**, *11*, 521–526.
- (25) Wang, H.-m.; Zhu, J.-y.; Ye, K.-b. Simulation, experimental evaluation and performance improvement of a cone dielectric elastomer actuator. *J. Zhejiang Univ.* **2009**, *10*, 1296–1304.
- (26) Liu, Y.; Tang, Z.; Wu, S.; Guo, B. Integrating Sacrificial Bonds into Dynamic Covalent Networks toward Mechanically Robust and Malleable Elastomers. *ACS Macro Lett.* **2019**, *8*, 193–199.
- (27) González, L.; Valentín, J. L.; Fernández-Torres, A.; Rodríguez, A.; Marcos-Fernández, A. Effect of the network topology on the tensile strength of natural rubber vulcanizate at elevated temperature. *J. Appl. Polym. Sci.* **2005**, *98*, 1219–1223.
- (28) Sherman, C. L.; Zeigler, R. C.; Verghese, N. E.; Marks, M. J. Structure-property relationships of controlled epoxy networks with quantified levels of excess epoxy etherification. *Polymer* **2008**, *49*, 1164–1172.
- (29) Mijovic, J.; Wijaya, J. Etherification Reaction in Epoxy-Amine Systems at High-Temperature. *Polymer* **1994**, *35*, 2683–2686.
- (30) Guerre, M.; Taplan, C.; Winne, J. M.; Du Prez, F. E. Vitrimers: directing chemical reactivity to control material properties. *Chem. Sci.* **2020**, *11*, 4855–4870.
- (31) Wang, S.; Teng, N.; Dai, J.; Liu, J.; Cao, L.; Zhao, W.; Liu, X. Taking advantages of intramolecular hydrogen bonding to prepare mechanically robust and catalyst-free vitriimer. *Polymer* **2020**, *210*, 123004.
- (32) Cuminet, F.; Caillol, S.; Dantras, E.; Leclerc, E.; Ladmira, V. Neighboring Group Participation and Internal Catalysis Effects on Exchangeable Covalent Bonds: Application to the Thriving Field of Vitriimer Chemistry. *Macromolecules* **2021**, *54*, 3927–3961.
- (33) Sheima, Y.; Yuts, Y.; Frauenrath, H.; Opris, D. M. Polysiloxanes Modified with Different Types and Contents of Polar Groups: Synthesis, Structure, and Thermal and Dielectric Properties. *Macromolecules* **2021**, *54*, 5737–5749.
- (34) Ni, Y. F.; Yang, D.; Wei, Q. G.; Yu, L. Y.; Ai, J.; Zhang, L. Q. Plasticizer-induced enhanced electromechanical performance of natural rubber dielectric elastomer composites. *Compos. Sci. Technol.* **2020**, *195*, 108202.